Analytical Biochemistry 423 (2012) 39–45

Contents lists available at SciVerse ScienceDirect

Analytical Biochemistry

journal homepage: www.elsevier.com/locate/yabio

Cell-free synthesis of cytochrome bo_3 ubiquinol oxidase in artificial membranes

Ahu Arslan Yildiz [a,b], Wolfgang Knoll [c], Robert B. Gennis [d], Eva-Kathrin Sinner [b,e,*]

[a] Max Planck Institute for Polymer Research, 55128 Mainz, Germany
[b] Institute of Materials Research and Engineering (IMRE), Singapore 117602, Singapore
[c] Austrian Institute of Technology (AIT), 1220 Vienna, Austria
[d] Department of Biochemistry, University of Illinois, Urbana, IL 61801, USA
[e] Department of NanoBioTechnologie (DNBT), University of Natural Resources and Applied Life Sciences (BOKU), 1190 Vienna, Austria

ARTICLE INFO

Article history:
Received 3 August 2011
Received in revised form 10 January 2012
Accepted 11 January 2012
Available online 20 January 2012

Keywords:
Cell-free protein synthesis
Cytochrome bo_3 ubiquinol oxidase
Electron transport chain
Mitochondrial disorders
Artificial membrane
Synthetic bioarchitectures

ABSTRACT

The analysis of membrane proteins is notoriously difficult because isolation and detergent-mediated reconstitution often results in compromising the protein structure and function. We introduce a novel strategy of combining a cell-free expression method for synthesis of a protein species coping with one of the most important obstacles in membrane protein research—preserving the structural–functional integrity of a membrane protein species and providing a stable matrix for application of analytical tools to characterize the membrane protein of interest. We address integration and subsequent characterization of the cytochrome bo_3 ubiquinol oxidase (Cyt-bo_3) from de novo synthesis without the effort of conventional cell culture, isolation, and purification procedures. The experimental output supports our idea of a suitable platform for in vitro protein synthesis and functional integration into a membrane-mimicking structure. We show the compatibility of different concepts of in vitro synthesis toward biosensor applicability by the example of Cyt-bo_3 protein expression. Our results obtained from in vitro synthesized proteins displayed similar behavior to proteins isolated from the cellular context. Overall, our approach is suitable for the in vitro expression of "complex" protein species such as Cyt-bo_3, which can be reproducible and stably synthesized and preserved in robust, synthetic planar membrane architecture.

It has been well documented that mitochondria are connected to several human diseases [1], broadly named as mitochondrial disorders [2,3]. The "electron transport chain" protein complexes are the key players in most of the mitochondrial diseases. Parkinson's disease [4] is the most frequent form of mitochondrial disorders. The reduced activity of complex I and complex IV of the respiratory chain is generally believed to be the causative agent of Parkinson's disease. It has been estimated that 80% of mitochondrial diseases are based on reduced activity of respiratory chain or dysfunction. Although general pathological pathways of mitochondrial disorders are known, the relation between structural features of respiratory chain complexes and their function remains unidentified.

The respiratory chain, also called the electron transport chain, is a series of four-membrane-bound protein complexes that are composed of multisubunit enzyme complex contributing ATP synthesis. Cytochrome *c* oxidase, namely complex IV, is the terminal enzyme of the respiratory chain in mitochondria, and it catalyzes the reduction of molecular oxygen to water. Cytochrome bo_3 ubiquinol oxidase (Cyt-bo_3)[1] is the bacterial homolog of the mammalian cytochrome *c* oxidase [5]. Several studies have been reported for respiratory chain proteins studying their function and structure [6–9]; however, functional in vitro expression of Cyt-bo_3 has not been reported yet.

In vivo expression and purification approaches were chosen to obtain the target protein species for characterization purposes. Taken together, membrane protein research to date is still suffering from not having a suitable experimental platform for structural and functional characterization; thus, few examples of membrane proteins have been characterized in suitable experimental platforms [10,11].

In this study, we combined two suitable approaches to maintain the structural and functional integrity of the membrane protein: (i) the artificial membrane technology in both planar and vesicular conformation and (ii) cell-free protein synthesis (CFPS). Mimics of biological membranes such as solid supported lipid membranes are widely used as a platform to investigate protein membrane

* Corresponding author at: Department of NanoBioTechnologie (DNBT), University of Natural Resources and Applied Life Sciences (BOKU), 1190 Vienna, Austria. Fax: +43 1 47891 12.
E-mail address: eva.sinner@boku.ac.at (E.-K. Sinner).

[1] *Abbreviations used:* Cyt-bo_3, cytochrome bo_3 ubiquinol oxidase; CFPS, cell-free protein synthesis; tBLM, tethered bilayer lipid membrane; SPFS, surface plasmon enhanced fluorescence spectroscopy; Ni–NTA, nickel–nitrilotriacetic acid; PBS, phosphate-buffered saline; SPR, surface plasmon resonance spectroscopy; 1°Ab, primary antibody; BSA, bovine serum albumin; IgG, immunoglobulin G; 2°Ab, secondary antibody; SDS–PAGE, sodium dodecyl sulfate–polyacrylamide gel electrophoresis; UQH_2, ubiquinol; SU II, subunit II of Cyt-bo_3; SU I, subunit I of Cyt-bo_3; SU III, subunit III of Cyt-bo_3; SU IV, subunit IV of Cyt-bo_3; PVDF, polyvinylidene fluoride.

0003-2697/$ - see front matter © 2012 Elsevier Inc. All rights reserved.
doi:10.1016/j.ab.2012.01.007

interactions [12–16]. The overall strategy is illustrated in Fig. 1, namely formation of tethered bilayer lipid membrane (tBLM) followed by in vitro expression of the aimed protein Cyt-bo_3.

The solid supported artificial membrane system provides a suitable platform for CFPS, in particular for membrane proteins [17]. The membrane structure is an essential factor for correct protein folding and functionality [18]. CFPS allows fast, reliable, and robust production of proteins of all kinds [19]. By combining these two approaches: CFPS and an artificial membrane system, we are able to address even complex membrane protein species, such as Cyt-bo_3, embedded inside the peptide supported membrane system. As a novel platform technology, we are exploring this combined system to create a model for cellular membranes mimicking membrane function, such as a target structure for protein insertion, stabilizing the protein function and, thus, enabling the analysis of ligand interactions. Protein insertion and orientation is detected by surface plasmon enhanced fluorescence spectroscopy (SPFS), presented in Fig. 1B. We observed that both membrane protein species and membrane architectures are tightly associated with each other and that the artificial membrane system has a pronounced effect on the expression and insertion process. Besides protein synthesis, determination of protein functionality is the other primary objective of this work. In most cases, functionality studies fail because protein-based approaches require a significant amount of protein-containing cofactors. However, our approach, in vitro expression of Cyt-bo_3 in artificial membrane structure, facilitates obtaining a considerable amount of protein that exhibits functionality. We are able to demonstrate the performance of the in vitro synthesized and membrane reconstituted Cyt-bo_3, comparing the physiological parameter (oxygen consumption) as a function of functionality.

Materials and methods

Strain information and in vivo expression

Escherichia coli strains containing pJRHisA plasmid-containing natural promoter [20,21] and pETcyo plasmid-containing T7 promoter [22] (gifts from R.B. Gennis, University of Illinois) were used in this study. Each plasmid encodes the cyoABCDE operon expressing Cyt-bo_3 with a 6 × His tag on the C terminus of subunit II. Recombinant Cyt-bo_3 samples were expressed in *E. coli* C43 as explained previously [20–23]. His-tagged protein was purified by using an Ni–NTA (nickel–nitrilotriacetic acid) Fast Start Kit (Qiagen, cat. no. 30600). Purification was carried out as explained in the QIAexpress Ni–NTA Fast Start manual. Purified protein was always used as a positive control in both expression and functionality studies.

The same media and procedure were applied to culture bacteria for plasmid extraction. High-quality plasmid DNA was prepared with a PureYield Plasmid Midiprep System (Promega, cat. no. A2492). Plasmid extraction was done by using the alkaline lysis method as indicated by the manual of the kit. Extracted plasmids were concentrated and purified by ethanol precipitation. Plasmid complementary DNA (cDNA) materials were used directly for in vitro expression.

Artificial membrane preparation

Self-assembly of the tBLM was carried out step by step as follows. First, assembly of 0.01 mg/ml α-laminin peptide (P19, Sigma, cat. no. C6171) as a spacer was done by incubating 50-nm-thick gold substrate for 45 min. Amine coupling reaction was completed in 10 min by using 0.4 M 1-ethyl-3-(3-dimethylaminopropyl) carbodiimide hydrochloride (EDC, Fluka, cat. no. 03449) and 0.1 M *N*-hydroxysuccinimide (NHS, Fluka, cat. no. 56480). This was followed by the addition of 0.2 mg/ml 1,2-dimyristoyl-*sn*-glycero-3-phosphoethanolamine (DMPE, Sigma, cat. no. P5693) as a monolayer, which solubilized in phosphate-buffered saline (PBS) with 0.1% Triton X-100 (Sigma, cat. no. T9284) and was incubated for 60 min. Next, 50-nm vesicles were prepared by using the extrusion method. Lipid solution was passed through the 50-nm polycarbonate membranes (Avestin). Formation of bilayer was achieved by the addition of 1.0 mg/ml 50-nm L-α-phosphatidylcholine (PC) vesicles (Fluka, cat. no. 61757), and vesicle spreading was completed in 90 min. This planar membrane structure was used for cell-free expression and SPFS experiments. For the SPFS experiments, a homemade surface plasmon resonance spectroscopy (SPR) setup (MPIP–Mainz) and a homemade flow cell in

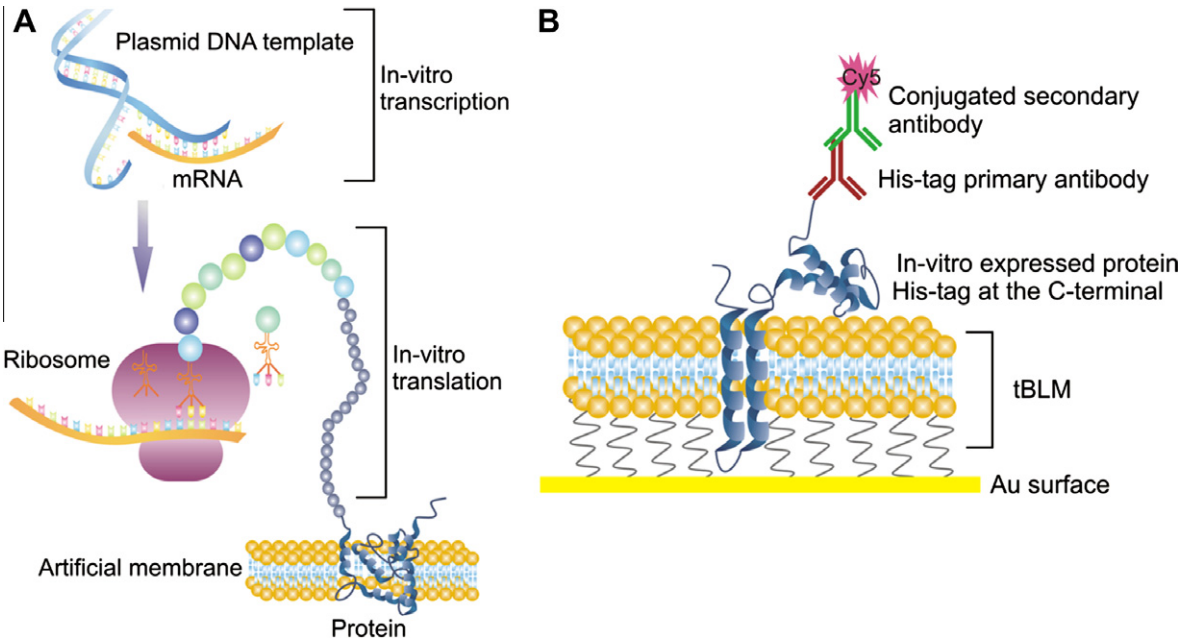

Fig.1. Schematic representation of in vitro expression of a membrane protein in an artificial membrane system (A) and membrane protein insertion that is detected by surface plasmon enhanced fluorescence spectroscopy (SPFS) through conjugated antibody sandwich system (B).

a Kretschmann configuration, which has a volume of 50 μl, was used.

In vitro expression of Cyt-bo_3 and detection via SPR/SPFS

An *E. coli* T7 S30 Extract System for Circular DNA (Promega, cat. no. L1130) was used for in vitro expression of Cyt-bo_3. Cell-free expression studies were performed as explained in the manual of the expression kit; all necessary components were mixed, and in vitro synthesis was initiated by adding the corresponding plasmid DNA. Incubation was done either in a test tube or in the SPFS flow cell at 37 °C for 2 h. A 50-μl flow cell was used each time for in vitro expression. For the SPFS experiments, a blocking strategy was applied for 1 h after in vitro expression. Next, 1 ml of 0.5% blocking solution (Roche, cat. no. 11921673001) was used to block unoccupied places on the membrane surface to prevent nonspecific antibody binding. Fluorescent labeling experiments were performed by using either a Penta-His Alexa Fluor 647-conjugated 1°Ab (primary antibody) labeling system (Qiagen, cat. no. 35370) or a Penta-His Ab (bovine serum albumin [BSA]-free) mouse monoclonal IgG (immunoglobulin G) 1°Ab (Qiagen, cat. no. 34660)/Cy5-conjugated secondary antibody goat–anti-mouse IgG H + L 2°Ab (secondary antibody) (Chemicon, cat. no. AP181S) sandwich complex. Either 200 μl of 2% Penta-His Ab (BSA-free) mouse monoclonal IgG 1°Ab and 3% Cy5-conjugated secondary antibody goat–anti-mouse IgG H + L 2°Ab solutions were added, respectively, or 200 μl of 3% Penta-His Alexa Fluor 647-conjugated 1°Ab solution was added and allowed to incubate for 45 to 60 min for fluorescent labeling. An SPFS scan was recorded after rinsing the system. All reactions and rinsing steps were carried out with PBS buffer.

All data were calculated from at least three independent measurements, and Origin Pro 7.5 software was used to calculate mean values. Baseline was subtracted from the fluorescence curve each time.

Analysis of in vitro and in vivo expressed Cyt-bo_3

Both in vivo and in vitro samples were analyzed by sodium dodecyl sulfate–polyacrylamide gel electrophoresis (SDS–PAGE) and the immunoblotting technique. An XCell SureLock chamber system (Invitrogen) was used for gel electrophoresis, an iBlot Dry Blotting system (Invitrogen) was used for the transfer of the gel to the membrane, and a WesternBreeze chemiluminescent kit/anti-mouse (Invitrogen, cat. no. WB7104) was used for chemiluminescent detection. Coomassie staining was done by using SimplyBlue staining reagent (Invitrogen, cat. no. LC6060). Sample preparations and all other reactions were carried out as explained in the system manuals. Acetone precipitation was done for in vitro samples to get rid of excess lipids from the system to remove background stains. After development of the membrane, Western blot images were obtained and bands were characterized by a LAS 3000 Imaging System (Fuji). For observation of His-tagged proteins, a 6 × His Protein Ladder (Qiagen, cat. no. 34705) was used as the His-tag marker and the same antibodies used in the SPFS system were used for development of the bands. The 6 × His protein ladder was used to calculate the concentration of in vitro synthesized samples. SDS–gel loading buffer, namely LDS buffer (Invitrogen, cat. no. NP0007), was used to solubilize the membrane components and integrated protein for further immunoblotting analysis of SPFS samples.

Functionality tests

In vitro expressed His-tag enzyme was purified by modifying previous methods [6,21]. After expression, 400 μl of expression mixture was suspended in 50 mM potassium phosphate (pH 8.3). In vitro extract residue was removed by centrifugation at 9000 rpm for 15 min (Eppendorf 5810R centrifuge) at 4 °C. Proteins were sedimented by centrifugation of supernatant at 47,000 rpm in a Beckman UltraMax ultracentrifuge at 4 °C for 3 h. The pellet was resuspended in 50 mM K_2HPO_4 (pH 8.3) and solubilized by the addition of Triton X-100 (1%) and octyl glucoside (1.25%). The solution was mixed for 1 to 2 h prior to solubilization of the pellet and was kept on ice. The solution was centrifuged again at 30,000 rpm and 4 °C for 20 min to remove all insoluble material. An Amicon Ultra–0.5 Centrifugal Filter (Millipore, cat. no. UF505024) was used to concentrate the final solution at 4500 rpm for 15 min. The concentrated protein solution was used for enzyme activity assay and SDS–gel analysis without further nickel affinity purification.

A YSI 5300A Oxygen Electrode Micro System (Yellow Life Sciences) with a 600-μl chamber was used for measurement of the oxygen consumption rate. Ubiquinone-1, namely coenzyme-Q (Sigma, cat. no. C7956), was used as an analog of substrate. Ubiquinone (UQ) was reduced as explained previously [19]. Substrate solutions were prepared in different concentrations varying from 50 to 500 μM ubiqinol (UQH_2) in 50 mM K_2HPO_4 buffer (pH 7.0). Cyanide binding data were obtained by the addition of 20 mM of the cyanide ligand to the oxidized enzyme prior to enzyme activity assay.

Results and discussion

SDS–gel analysis of Cyt-bo_3 samples

In vitro expression of Cyt-bo_3 followed by the insertion into artificial membrane surface was confirmed by Western blot analysis for both pJRHisA (Fig. 2A) and pETcyo (Fig. 2B) clones. Here, we discuss two critical issues: in vitro expression of the target protein and its insertion into the artificial membrane. To ascertain the in vitro expression of Cyt-bo_3, a series of Western blot analyses had been performed. Previously expressed and purified in vivo protein [5,6] was used as a reference (Figs. 2A and B, lane 2). Lane 3 in Fig. 2A and lane 4 in Fig. 2B indicate the cell-free expression of Cyt-bo_3 by formation of double bands at 33 to 35 kDa. This double band behavior is a consequence of signaling peptide cleavage of the subunit II (SU II) from the N terminus. Previously reported data [24] for in vivo expressed protein show that the size of the uncleaved SU II is 35 kDa, whereas that of the cleaved protein is 33 kDa. Whole Western blot analysis shows that Cyt-bo_3 can be successfully expressed in an artificial membrane system.

In addition, Fig. 2C shows the Coomassie blue staining of in vitro expressed Cyt-bo_3 samples for pETcyo plasmid. Corresponding bands of four subunits (SU I, SU II, SU III, and SU IV) indicate the in vitro expression of Cyt-bo_3 and assembly of all subunits (Fig. 2C, lane 5). Lanes 2 and 3 represent the in vitro extract after synthesis without further purification for the negative control (no DNA added) and the Cyt-bo_3 sample, respectively. After purification, in vitro synthesized Cyt-bo_3 (lane5) exhibits corresponding bands for each subunit, which is not the case for the negative control (lane 4). Extra bands might originate from dimerization of subunits as reported previously [25].

To analyze the effect of various expression mixtures on expression level, different expression systems have been characterized in parallel. An Insect Expression Kit (Qiagen), a TNT Quick Coupled System/reticulocyte lysate (Promega), and a TNT Wheat Germ Expression System (Promega) were examined. Expression of Cyt-bo_3 was not achieved by using these expression mixtures (data not shown). These expression systems were chosen because of their capability to synthesize eukaryotic proteins or complex proteins with posttranslational modifications. No expression was observed for both plasmids, clearly indicating that in vitro synthesis was disrupted by some factors. At this point, failure of Cyt-bo_3

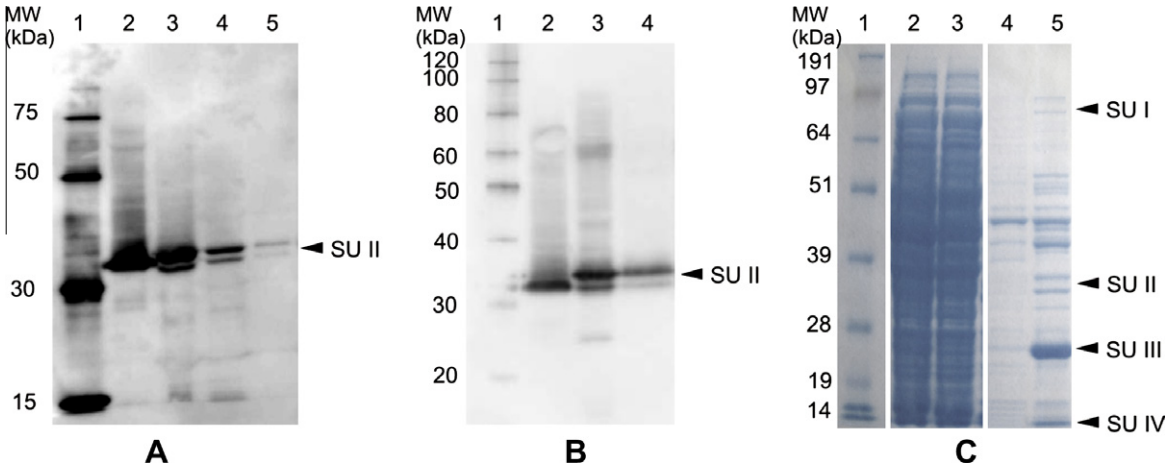

Fig.2. (A) Representative SDS–PAGE gel of Cyt-bo_3 expressed by using pJRHisA plasmid. Lane 1: His-tag protein ladder; lane 2: in vivo expressed Cyt-bo_3; lanes 3 and 4: in vitro expressed Cyt-bo_3; lane 5: solubilized Cyt-bo_3 collected from membrane. (B) Representative SDS–PAGE gel of Cyt-bo_3 expressed by using pETcyo plasmid. Lane 1: benchmark chemiluminescent marker; lane 2: in vivo expressed Cyt-bo_3; lane 3: in vitro expressed Cyt21 bo_3; lane 4: solubilized Cyt-bo_3 collected from membrane. (C) Coomassie blue staining of Cyt-bo_3 expressed by using pETcyo plasmid. Lane 1: See Blue Plus 2 marker; lane 2: negative control (no DNA) in vitro extract without any purification; lane 3: in vitro expressed Cyt-bo_3 without any purification; lane 4: negative control sample after purification; lane 5: in vitro expressed Cyt-bo_3 after purification. (NuPAGE Novex 10% Bis–Tris gel, 200 V, 50 min, Mops buffer, polyvinylidene fluoride [PVDF] membrane, WesternBreeze chemiluminescent anti-mouse system). (For interpretation of the references to colour in this figure legend, the reader is referred to the web version of this article.)

expression for pJRHisA plasmid could be due to the lack of T7 promoter. It is known [26,27] that pJRHisA plasmid has an intrinsic promoter sequence that works with the *E. coli* expression system; however, the intrinsic promoter does not appear to be compatible with other expression systems; thus, no expression product was obtained in detectable amounts for functional characterization. Although pETcyo plasmid contains the well-known T7 promoter, it did not produce any expression product either. We interpret this observation as employing T7 promoter and the *E. coli* cell-free system as the optimal match in terms of expression of the Cyt-bo_3, and heading toward a completely different system from the target protein's nature is not favored, which is found for cell-based systems as well.

Detecting in vivo expressed Cyt-bo_3 insertion by SPFS after expression and purification processes

For the detection of Cyt-bo_3, the SPFS method [28] was chosen to enhance the detection limit of the optical sensor device that is based on evanescent wave techniques such as SPR [29]. Here, two approaches were followed to detect Cyt-bo_3 via antibody–protein interaction. The first route was the "sandwich assay," which uses primary and secondary antibodies to detect the target protein. The 1°Ab (Penta-His Ab) was directed against target protein Cyt-bo_3, and labeled 2°Ab (Cy5 conjugate) was directed against 1°Ab. As a second route, labeled 1°Ab (Penta-His Alexa Fluor 647 conjugate) was used directly against Cyt-bo_3. The reason for choosing Alexa Fluor 647-labeled 1°Ab was to prevent misinterpretation that may be caused by multiple binding of 2°Ab. Moreover Alexa Fluor 647 conjugate shows higher stability for a longer incubation period, which increases the binding efficiency.

We examined the possibility of integration of in vivo expressed and purified Cyt-bo_3 into an artificial membrane. An artificial membrane system was incubated with 100 μl of purified and concentrated Cyt-bo_3 that was expressed in vivo by using pJRHisA plasmid (Fig. 3) as the "blueprint." An SPFS signal was detected after applying the in vivo synthesized Cyt-bo_3 protein into the artificial membrane system without blocking solution. Integration of in vivo expressed Cyt-bo_3 did not produce a detectable SPFS signal when the blocking solution was used, indicating that insertion of in vivo synthesized Cyt-bo_3 does not happen under these conditions and that obtained signal comes only from unspecific binding of antibodies. This is not a surprise given that Cyt-bo_3 is complex and a big membrane protein.

Detecting in vitro expression of Cyt-bo_3 in presence of artificial membrane system

Results reported in the previous section support our theory and show that while expressing membrane proteins, they favor the presence of membrane structures for integration and folding.

In vitro expression and insertion of Cyt-bo_3 was determined via the SPFS method. Typical angular fluorescent scan curves were presented for in vitro expression mixture containing pJRHisA (Fig. 4A) and pETcyo (Fig. 4B) plasmid DNA. In each figure, fluorescent curves correspond to two different labeling system: Alexa Fluor 647 and Cy5. Fluorescent maxima of both systems were in the same range and same order of magnitude for products of both pJRHisA plasmid and pETcyo. In addition, negative control that has no DNA or gene of interest was presented in the same figures to prove that the signal is originating from expressed and integrated membrane protein.

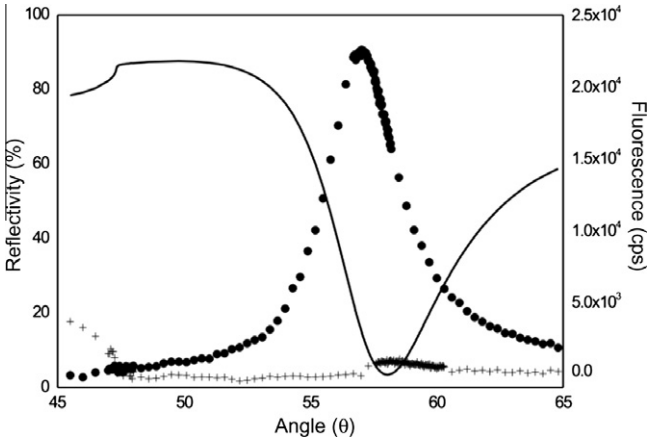

Fig.3. SPFS results for insertion behavior of in vivo expressed and purified Cyt-bo_3 observed by the following: (●) Penta-His 1°Ab/Cy5-conjugated 2°Ab labeling system; (+) negative control; (—) SPR scan curve.

It must be noted that the antibodies employed have a high affinity to bind membrane surface unspecifically; therefore, a blocking strategy (as described in Materials and methods) was applied every time after in vitro expression of the target protein to block unoccupied sites on the membrane surface. Significant difference in fluorescent signal intensity between in vitro samples and their negative controls is a common feature in both Figs. 4A and B, indicating that the cell-free expression of Cyt-bo_3 and its integration in the membrane was successfully achieved. Detected fluorescent intensity was 5.0 to 6.5 $\times$ 10^5 cps for the product of pETcyo plasmid (Fig. 4B), whereas it was 2.5 to 3.5 $\times$ 10^4 cps for the product of pJRHisA plasmid (Fig. 4A). Resulting fluorescence maxima of angular scan curves of pETcyo plasmid (Fig. 4B) were 10-fold higher than the signal detected with pJRHisA plasmid. The presence of T7 promoter in pETcyo plasmid makes a significant difference in the expression level and efficiency given that the expression system was compatible with T7 promoter systems.

SDS–gel analysis for detection of Cyt-bo_3 insertion

To further strengthen the evidence of Cyt-bo_3 insertion during in vitro expression, corresponding SPFS samples were further analyzed by using the SDS–gel method. It was challenging to observe the integration of Cyt-bo_3 in the artificial membrane system. In this study, characterization was mainly done by SPR/SPFS. SPR provides information about increases in optical mass; however, no specificity is involved, and SPR is not capable of probing protein insertion into membrane. Because the artificial membrane/expression system has many components, obtained signal can be originating from either inserted or attached layer of protein. To provide evidence for insertion of target protein, artificial membrane and its contents were solubilized with LDS buffer that contains strong detergents and reducing agents. The resulting solution should contain solubilized in vitro Cyt-bo_3 that had been integrated in artificial membrane. Bulk cell-free expression mixture rinsed from membrane surface (Figs. 2A and B, lane 3) and solubilized protein samples (Fig. 2A, lane 5, and Fig. 2B, lane 4) were compared for the same experimental run. Treating the membrane and its components with LDS buffer yields distinct bands typical for the Cyt-bo_3 for each plasmid (Fig. 2A, lane 5, and Fig. 2B, lane 4). Observed bands clearly indicate that protein is integrated into the membrane. Expression yield and amount of inserted product can be seen and observed roughly from the intensity of the bands. The most promising result is the one with improved band intensity of solubilized membrane product for pETcyo plasmid (Fig. 2B, lane 4), meaning higher expression and integration yield.

Enzyme activity

We further characterized the functionality of in vitro expressed Cyt-bo_3 and compared its kinetic values with those expressed via in vivo synthesis in the conventional cell-based method [20–22,30]. The presence of in vitro synthesized protein was shown by ultraviolet–visible (UV–Vis) spectra. The main limitation of the in vitro expression system is the small amount of synthesized protein product. Therefore, only the mere absorption behavior of proteins was investigated at around 280 nm instead of the characteristic "reduced minus oxidized" spectra of Cyt-bo_3 [21]. Absorption maxima were observed at 262 or 263 nm for both pETcyo and pJRHisA in vitro products (Fig. 5), and the background effect of only the cell-free expression extract was used as a negative control because the cell-free extract is a protein mixture itself. It was clearly observed that there was a significant absorbance difference between negative control, which is only the cell-free extract itself (containing no DNA), and in vitro expression samples for both pJRHisA and pETcyo plasmids. Another substantial finding regarding the absorbance values was as expected, namely that the cell-free expression efficiency of pETcyo plasmid is higher than that of pJRHisA plasmid.

For better quantitative analysis, concentrations of cell-free expression products were investigated by using the Western blot technique (Fig. 6) shown in Table 1. In vitro synthesized enzyme concentrations were calculated from the intensities of Western blot bands by using Aida Image Analyzer software. The 6 $\times$ His protein ladder was used as a positive control for calculation of total enzyme amount by means of His-tagged product. The first lane in Fig. 6 (lane a) represents the 6 $\times$ His protein ladder, and intensity of the 30-kDa band (number 1) corresponds to 100 ng of His-tagged protein per 5-µl sample. Regarding the in vitro expression products, the second lane in Fig. 6 (lane b) represents the pETcyo expression product, and the third lane (lane c) belongs to pJRHisA product. The band labeled as number 2 is the uncleaved His-tagged SU II, which is exactly 63.1 ng of Cyt-bo_3/µl, and number 3 is the cleaved His-tagged SU II of Cyt-bo_3, which corresponds to 15.9 ng of Cyt-bo_3/µl. Evaluation of Western blot analysis (Table 1) emphasized once more that the expression yield of pETcyo is always higher than that of pJRHisA plasmid (number 4) due to the T7 promoter. Here, it was shown in detail that the concentration of the uncleaved protein is always higher than that of the cleaved protein.

The enzymatic activity of Cyt-bo_3 was estimated by measuring consumption of oxygen for ubiquinol oxidation. Ubiquinol-1 oxidation rates were measured with the oxygen electrode micro

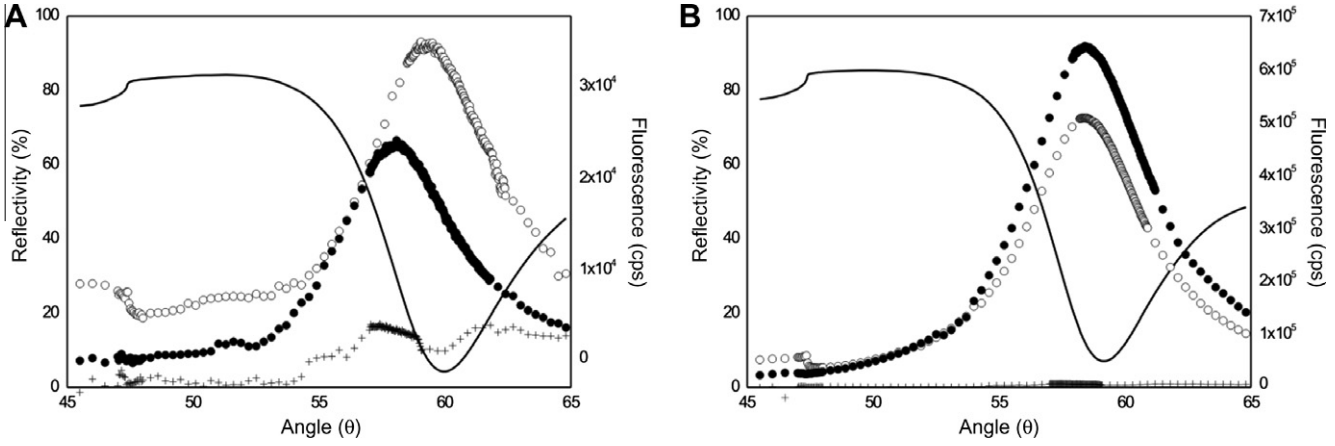

Fig.4. (A) SPFS measurements of in vitro expression of Cyt-bo_3 (pJRHisA plasmid) observed by the following: (○) Alexa Fluor 647-conjugated 1°Ab system; (●) Penta-His 1°Ab/Cy5-conjugated 2°Ab labeling system; (+) negative control; (—) SPR scan curve. (B) SPFS measurements of in vitro expression of Cyt-bo_3 (pETcyo plasmid) observed by the following: (○) Alexa Fluor 647-conjugated 1°Ab system; (●) Penta-His 1°Ab/Cy5-conjugated 2°Ab labeling system; (+) negative control; (—) SPR scan curve.

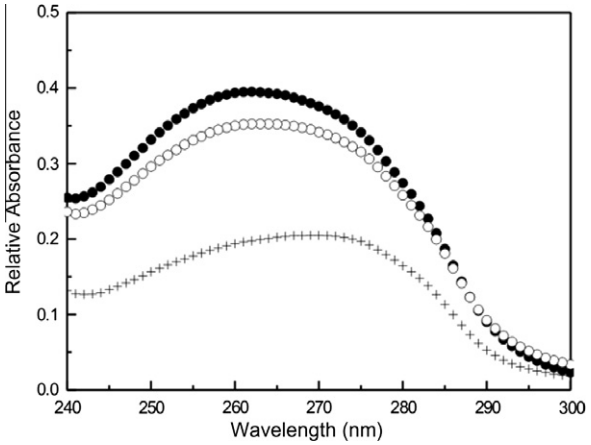

Fig.5. Spectrophotometric properties of in vitro expressed Cyt-bo_3 by the following: (●) pETcyo plasmid; (○) pJRHisA plasmid; (+) negative control.

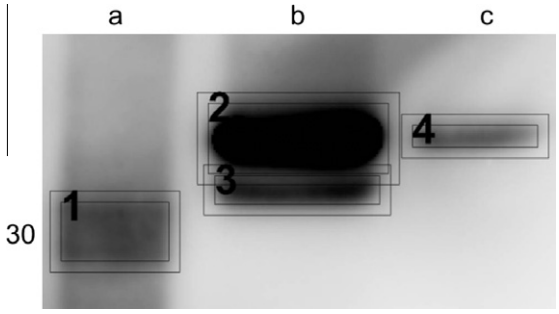

Fig.6. Representative Western blot analysis for concentration determination of the following: (a) signal, derived from the His-tag protein ladder, indexed with number 1; (b) in vitro synthesized Cyt-bo_3 from pETcyo plasmid Cyt-bo_3, labeled with numbers 2 and 3; (c) in vitro synthesized Cyt-bo_3 from pJRHisA plasmid (labeled with number 4). (NuPAGE Novex 10% Bis–Tris gel, 200 V, 50 min, Mops buffer, PVDF membrane, WesternBreeze chemiluminescent anti-mouse antibody system).

Table 1
In-vitro expressed Cyt-bo_3 concentrations for pJRHisA and pETcyo plasmid.

In vitro product	Expression volume (μl)	Enzyme amount (ng Cyt-bo_3/μl)
pJRHisA Cyt-bo_3	350	9.1
pETcyo Cyt-bo_3	400	79.0

system. The in vitro expressed and purified pJRHisA Cyt-bo_3 concentration was 349 fmol, and it was below the detection limit of the oxygen electrode system; thus, pETcyo Cyt-bo_3 was used to observe enzymatic activity of in vitro expression product. Oxygen consumption signals of in vitro expressed and purified pETcyo Cyt-bo_3 are given in Fig. 7 for two different concentrations of ubiquinol: 400 and 500 μM UQH_2, 6.1 pmol, 10 μl of Cyt-bo_3 solution. In vitro extract that was prepared without DNA was used as a negative control to check on the possibility of oxygen consumption by other components or impurities. The resulting negative control curve was at nearly the same level of the baseline (Fig. 7). In addition, cyanide binding behavior was examined for the purified in vitro Cyt-bo_3 to provide evidence of functionality. The enzyme sample was treated with 20 mM cyanide ligand prior to detecting the enzyme activity for 500 μM UQH_2, resulting in an inhibitory effect of cyanide that is shown in Fig. 7.

The specific ubiquinol activity of in vitro expressed pETcyo Cyt-bo_3 is 0.1 μmol/min/mg at 25 °C and 400 μM UQH_2. The specific activity of the in vitro sample is slightly less than native or Ni–NTA purified counterparts; nevertheless, in vitro Cyt-bo_3 activity

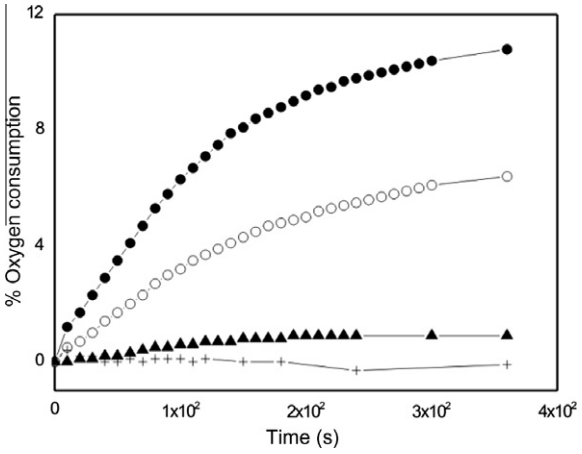

Fig.7. Oxygen consumption measurement for *in-vitro* synthesized and purified pETcyo Cyt-bo_3 (6.1 pmol, 10 μl Cyt-bo_3) (●) 500 μM UQH_2; (○) 400 μM UQH_2; (▲) cyanide inhibition of Cyt-bo_3 for 500 μM UQH_2; (+) negative control.

is similar to that of the cytoplasmic membrane samples [21]. It is likely that without further ion exchange purification, in vitro Cyt-bo_3 sample behaves like the solubilized form of the enzyme associated with lipid membrane. Overall functionality tests clearly demonstrate that in vitro Cyt-bo_3 exhibits enzymatic activity.

Conclusion

The primary aim of this study was to develop a capable membrane/protein expression system for the functional synthesis of Cyt-bo_3, enabling the characterization of the membrane protein outside the complexity of a cellular membrane system. Our artificial lipid membrane system approach has successfully resulted in synthesis of functional Cyt-bo_3 embedded into an artificial lipid membrane structure. As a control experiment, integration behavior of in vivo expression product was examined in great detail. We observed that Cyt-bo_3 insertion does not occur if protein is synthesized outside the planar membrane structure. Therefore, we propose that the presence of artificial membrane is an optimal platform for synthesis and insertion of the Cyt-bo_3 and that the integration process probably needs a stimulus that starts directly on the membrane surface.

In addition, various expression mixtures and different clones were examined to elucidate their influences and dependency on in vitro synthesis, thereby investigating the boundary conditions of the synthesis. In this work, in vitro expression followed by integration in artificial membrane structure was achieved and showed that even large four-subunit membrane proteins can be successfully incorporated. We identified that T7 promoter with the *E. coli* cell-free extract is an optimal combination for the high-level expression of Cyt-bo_3, whereas other expression systems such as insect extract do not produce the target protein.

SPFS measurements of both pJRHisA and pETcyo plasmids showed that expression of Cyt-bo_3 using *E. coli* extract were successful. Corresponding Western blot analysis from SPFS samples provided further evidence of the expression and insertion of Cyt-bo_3 into the artificial membrane system. Overall, when pETcyo plasmid was used, the production yield of protein was higher and this was clearly confirmed via SPFS.

Furthermore, we aimed to develop a novel expression strategy for the application of functional studies. Despite the limited amount of in vitro expression product, it is still sufficient to explore the functionality of the Cyt-bo_3 complex, indicating correct insertion and, to a certain extent, correct protein folding as well. The oxygen consumption rate is presented here as a proof of function

for the pETcyo Cyt-bo_3. In addition, inhibition by cyanide binding supports functional studies. Compared with literature data [21], our results are in good agreement regarding the UQH_2 oxidation rate. Although use of the artificial membrane approach does not produce equivalent amounts of desired material yet, compared with in vivo expression, the purity and label-free synthesis provide functional integrated membrane protein while discarding tedious separation and purification steps.

The current method of in vitro expression of membrane proteins in artificial membranes represents a new concept toward potential device applications. One of the most challenging issues is still the production of functional membrane proteins and subsequent functionality studies. Consequently, this approach could be further extended for device application, quantifying protein characterization, because synthetic proteins can be employed in a defined context, allowing an optimal signal-to-noise ratio in characterizing specific membrane proteins outside the complexity of a living cell.

References

[1] R.W. Taylor, D.M. Turnbull, Mitochondrial DNA mutations in human disease, Nat. Rev. Genet. 6 (2005) 389–402.

[2] M. Zeviani, S. Di Donato, Mitochondrial disorders, Brain 127 (2004) 2153–2172.

[3] A. Gardner, R.G. Boles, Is a ''mitochondrial psychiatry'' in the future?, Curr Psychiatry Rev. 1 (2005) 255–271.

[4] T.B. Sherer, R. Betarbet, J.T. Greenamyre, Environment, mitochondria, and Parkinson's disease, Neuroscientist 8 (2002) 192–197.

[5] R.B. Gennis, Some recent advances relating to prokaryotic cytochrome *c* reductases and cytochrome *c* oxidases, Biochim. Biophys. Acta 1058 (1991) 21–24.

[6] J.A. Garcia-Horsman, B. Barquera, J. Rumbley, J. Ma, R.B. Gennis, The superfamily of heme-copper respiratory oxidases, J. Bacteriol. 176 (1994) 5587–5600.

[7] S. Riisama, Structural and Functional Studies of Bacterial Heme-Copper Oxidases, University of Helsinki, Academic dissertation, 2000.

[8] J. Abramson, S. Riistama, G. Larsson, A. Jasaitis, M. Svensson-Ek, L. Laakkonen, A. Puustinen, S. Iwata, M. Wikström, The structure of the ubiquinol oxidase from *Escherichia coli* and its ubiquinone binding site, Nat. Struct. Biol. 7 (2000) 910–917.

[9] R.G. Efremov, R. Baradaran, L.A. Sazanov, The architecture of respiratory complex I, Nature 27 (2010) 428–429.

[10] E.K. Sinner, W. Knoll, Functional tethered membranes, Curr. Opin. Chem. Biol. 5 (2001) 705–711.

[11] F. Giess, M.G. Friedrich, J. Heberle, R. Naumann, The protein-tethered lipid bilayer: a novel mimic of the biological membrane, Biophys. J. 87 (2004) 3213–3220.

[12] W. Knoll, I. Köper, R. Naumann, E.K. Sinner, Tethered bimolecular lipid membranes: a novel model membrane platform, Electrochim. Acta 53 (2008) 6680–6689.

[13] A.A. Brian, H.M. McConnell, Allogeneic stimulation of cyto-toxic T-cells by supported planar membranes, Proc. Natl. Acad. Sci. USA 81 (1984) 6159–6163.

[14] E. Sackmann, Supported membranes: scientific and practical applications, Science 271 (1996) 43–48.

[15] S. Goennenwein, M. Tanaka, B. Hu, L. Moroder, E. Sackmann, Functional incorporation of integrins into solid supported membranes on ultrathin films of cellulose, Biophys. J. 85 (2003) 646–655.

[16] M. Tanaka, E. Sackmann, Polymer-supported membranes as models of the cell surface, Nature 437 (2005) 656–663.

[17] R. Robelek, E.S. Lemker, B. Wiltschi, V. Kirste, R. Naumann, D. Oesterhelt, E.K. Sinner, Incorporation of in vitro synthesized GPCR into a tethered artificial lipid membrane system, Angew. Chem. Int. Ed. 46 (2007) 605–608.

[18] J.U. Bowie, Solving the membrane protein folding problem, Nature 438 (2005) 581–589.

[19] J.R. Swartz, Universal cell-free protein synthesis, Nat. Biotechnol. 27 (2009) 731–732.

[20] J.N. Rumbley, E. Furlong Nickels, R.B. Gennis, One-step purification of histidine-tagged cytochrome bo_3 from *Escherichia coli* and demonstration that associated quinone is not required for the structural integrity of the oxidase, Biochim. Biophys. Acta 1340 (1997) 131–142.

[21] J. N. Rumbley, Analysis of heme-copper ligation, quinol activity, and ligand binding kinetics of cytochrome bo_3 quinol oxidase from *E. coli*, Dissertation thesis, University of Illinois at Urbana–Champaign, 1995.

[22] H.L. Frericks, D.H. Zhou, L.L. Yap, R.B. Gennis, Magic-angle spinning solid-state NMR of a 144 kDa membrane protein complex: *E. coli* cytochrome bo_3 oxidase, J. Biomol. NMR 36 (2006) 55–71.

[23] J.S. Rieske, Preparation and properties of DPNH–coenzyme Q reductase, Method Enzymol. 10 (1967) 235–239.

[24] J. Ma, A. Katsonouri, R.B. Gennis, Subunit II of the cytochrome bo_3 ubiquinol oxidase from *Escherichia coli* is a lipoprotein, Biochemistry 36 (1997) 11298–11303.

[25] F. Stenberg, G. Von Heijne, D.O. Daley, Assembly of the cytochrome bo_3 complex, J. Mol. Biol. 371 (2007) 765–773.

[26] V. Chepuri, R.B. Gennis, The use of gene fusions to determine the topology of all of the subunits of the cytochrome *o* terminal oxidase complex of *Escherichia coli*, J. Biol. Chem. 265 (1990) 12978–12986.

[27] J. van der Oost, A.M. Lappalainen, A. Warne, L. Lemieuxl, J. Rumbley, R.B. Gennis, R. Aasa, T. Pascher, B.G. Malmstrom, M. Saraste, Restoration of a lost metal-binding site: construction of two different copper sites into a subunit of the *E. coli* cytochrome *o* quinol oxidase complex, EMBO J. 11 (1992) 3209–3217.

[28] J.W. Attridge, P.B. Daniels, J.K. Deakon, G.A. Robins, G.P. Davidson, Sensitivity enhancement of optical immunosensors by the use of a surface plasmon resonance fluoroimmunoassay, Biosens. Bioelectron. 6 (1991) 201–214.

[29] H. Raether, Surface Plasmon on Smooth and Rough Surfaces and on Gratings, Springer, Berlin, 1988.

[30] L.L. Yap, M.T. Lin, H. Ouyang, R.I. Samoilova, S.A. Dikanov, R.B. Gennis, The quinone-binding sites of the cytochrome bo_3 ubiquinol oxidase from *Escherichia coli*, Biochim. Biophys. Acta 1797 (2010) 1924–1932.